Study of the interdiffusion in Cu/Ni multilayer thin films by Auger electron spectroscopy depth profiling

X.L. Yan [1], Y. Liu [2], H.C. Swart [1], J.Y. Wang [2], J.J. Terblans [1]*

[1] Department of Physics, University of the Free State, PO Box 339, Bloemfontein, 9300, South Africa

[2] Department of Physics, Shantou University, 243 Daxue Road, Shantou, 515063 Guangdong, China

E-mail: terblansjj@ufs.ac.za

Abstract: The interdiffusion upon annealing of Cu/Ni multilayer structures at 325 ºC, 350 ºC and 375 ºC for 30 min was studied by Auger electron spectroscopy (AES) depth profiling. The measured AES depth profiles of the unannealed and annealed samples were quantitatively fitted by the MRI model and the interdiffusion parameters, pre-exponential factor D_o and activation energy E_a, were extracted. The depth-dependence of the interdiffusion coefficient in the Cu/Ni multilayer structures was characterized with relating to the reduction of the activation energy at deeper depth during sputtering.

1. Introduction

Multilayer thin films have been increasingly used in both basic research and applications because of their specific properties that differ from those of bulk materials and single-layer thin films [1]. The interdiffusion at interfaces has a strong impact on the properties of a multilayer thin-film system [2]. In addition, diffusion in polycrystalline thin films is much faster than in bulk materials due to a high density of defects such as dislocations, vacancies, and grain boundaries, which act as a short-cut for diffusion. So diffusion in polycrystalline thin films cannot be described by the extrapolation of data obtained for bulk materials at higher temperatures.

The Auger electron spectroscopy (AES) depth profiling technique is one of the most commonly used methods for the study of diffusion in multilayer thin films due to its high surface sensitivity. In the past decades, several methods have been proposed to extract the interdiffusion coefficient from AES depth profiling data. For example: the plateau-rise method [3], the center-gradient method [4], and the interface-width method [5] for a bilayer sample and a Fourier series method for a multilayer sample [6]. In these four methods, only parts of the measured depth profile are used for extracting the interdiffusion coefficient values. Recently, based on the Mixing-Roughness-Information depth (MRI) model [7], a new method for fitting the entire measured AES depth profile has been proposed [8] and widely been used to extract the interdiffusion coefficient in layered structures [9,10]. The aim of this study was to determine the interdiffusion coefficients in the Cu/Ni multilayer structures from measured AES depth profiling data by the MRI model.

* To whom any correspondence should be addressed.

2. Experimental

2.1. Sample preparation and annealing

The Ni/Cu multilayer structures, composed of four pairs of Ni and Cu layers, were prepared by electron beam physical vapour deposition onto passivated silicon (100) substrates (SiO_2) at a base pressure of $<9.3\times10^{-4}$ Pa, resulting in polycrystalline multilayer thin films. The passivated silicon (100) substrates (SiO_2) was the barrier layer for preventing diffusion into the substrates. The Ni layer films were deposited at a rate of ~0.2 nm/s, while the Cu layer films were deposited at a rate of ~0.3 nm/s. The layer thickness was monitored by an Inficom XTC thin film monitor as being Cu(8 nm)/Ni(8 nm)/Cu(11 nm)/Ni(11 nm)/Cu(15 nm)/Ni(12 nm)/Cu(13 nm)/Ni(14 nm)/SiO_2. Then the samples were annealed at 325 ^{o}C, 350 ^{o}C and 375 ^{o}C for 30 min, respectively in a high vacuum system ($< 5\times10^{-5}$ Pa).

2.2. AES depth profiling measurement

The depth profiles of the unannealed and annealed samples were measured using a PHI 600 Scanning Auger Microscope (SAM) without sample rotation at a base pressure $< 1.3\times10^{-7}$ Pa. A static primary electron beam of 10 keV and a beam current of 200 nA was used. The samples were sputtered employing 2 keV Ar^+ ions, incidence at an angle of 60^o, beam current density of 0.127 A/m^2 with a 2×2 mm^2 raster. The Auger peak-to-peak heights (APPH) were recorded as a function of sputtering time for Ni(680-740 eV), Cu(880-989 eV), C(240-295 eV), O(480-510 eV) and Si(70-105 eV). The average sputter rate of the Cu/Ni multilayers was 0.05 nm/s, as determined by depth profiling data of the unannealed sample with known thicknesses of the Cu/Ni layers.

2.3. Conversion of the intensity-sputter time profile into a normalized APPH depth profile

In order to apply the MRI model, the APPH-sputter time profiles were converted into normalised APPH depth profiles. According to the standard Auger spectra of pure Cu and Ni [11], the whole range of Ni and Cu Auger peaks overlapped except for the Cu 922 eV peak. The Cu APPH was normalized to the maximum of the Cu 922 eV APPH in the unannealed sample. The time scale was converted into the depth scale using the average sputtering rate of 0.05 nm/s (see previous paragraph). Conversions of the normalised APPH-sputter time profiles are shown in Fig.1 for the unannealed and annealed samples.

3. Results and discussion

For the unannealed sample, the normalised APPH of Cu depth profiling data and the best fit to the measured data by the MRI model are shown in Fig. 1(a) as open circles and a solid line, respectively. The atomic mixing length w is estimated as 1.0 nm by the TRIM code [12] and the Auger electron escape depth λ (effective attenuation length times cos(θ), where θ is the angle of emission of the detected electrons) for Cu (922 eV) is calculated as 0.8 nm [13]. The fitted roughness parameter, assumed as a linear increase with depth in the Cu/Ni polycrystalline multilayer structure, is obtained as $\sigma_0 = (0.9+0.049\times z)$ nm, which agrees very well with the AFM measured data in Ref.[14]. In addition, Fig. 1(a) shows that the measured Cu concentration in the near substrate region is lower than that in the near surface region due to ion beam sputter-induced roughness, same as that in depth profiling of Cu/Pd, Ag/Pd polycrystalline multilayer films [15, 16].

The unannealed Cu layered structure is also shown as a dashed line in Fig. 1(a). For the annealed samples, the normalised APPH Cu depth profiling data and the best fit to the measured data are shown in Fig. 1(b-d). The fitting parameters w and λ were kept the same as for the unannealed sample and only the roughness parameter was changed. The determined linear depth dependence of the roughness parameter σ, at the different temperatures, has been indicated in Fig. 1(b-d), respectively.

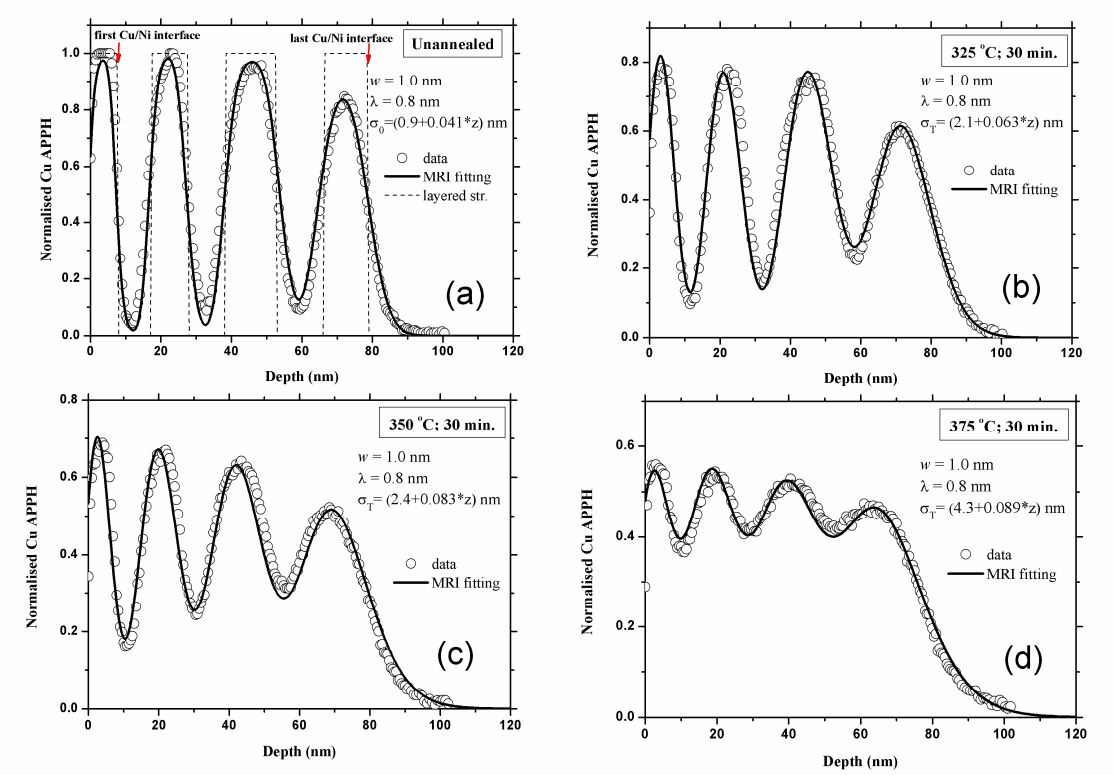

Figure 1. The normalised Cu depth profiling data and the best fit to the measured data by the MRI model for (a) the unannealed sample, and the annealed samples for 30 min at (b) 325 ºC (c) 350 ºC and (d) 375 ºC. The dashed line drawn in Fig. 1(a) represents the unannealed Cu sublayer structure.

According to the MRI model, the interface roughness broadening is described by a Gaussian function ~exp[-$z^2/2\sigma^2$] [7]. In an initial stage of diffusion, the diffusion-induced concentration profile can be written as a Gaussian function ~exp[-z^2/4Dt], where z represents the diffusion depth and the diffusion length is $(4Dt)^{1/2}$. Therefore, the square of the diffusion length can be expressed in terms of the interface roughness as [17]:

$$2Dt = \sigma_T^2 - \sigma_o^2 \qquad (1)$$

where t is the annealing time, and σ_T and σ_o are the values of the roughness parameter after and before annealing at temperature T, respectively. Using Eq. (1), the interdiffusion coefficient D can be determined from the fitted interface roughness parameter by the MRI model. Using the roughness parameter values presented in Figs. 1(a-d), the calculated values of the interdiffusion coefficient according to Eq. (1) at the two locations, namely at the first and the last Cu/Ni interface as indicated in Fig.1(a), are presented in Fig. 2 by open and solid circles, respectively. The corresponding values of the interdiffusion parameters, the pre-exponential factor D_o and the activation energy E_a determined from the Arrhenius plot are indicated in Fig. 2 and are compared with the literature values listed in Table1.

The interdiffusion in the Cu/Ni multilayer at the first Cu/Ni interface was determined as 6.2×10^{-13}exp(-101.4 *kJ/RT*) m^2/s, and at the last Cu/Ni interface as 6.3×10^{-14}exp(-79.0 *kJ/RT*) m^2/s. The dash-dotted line shown in Fig. 2 was also obtained from measured AES depth profiling data for Cu/Ni multilayer (m) films deposited on glass substrates [19]. The dashed line shown in Fig. 2 was obtained for a Cu(~100 nm)/Ni(~500 nm) bilayer (b) films sample [20].

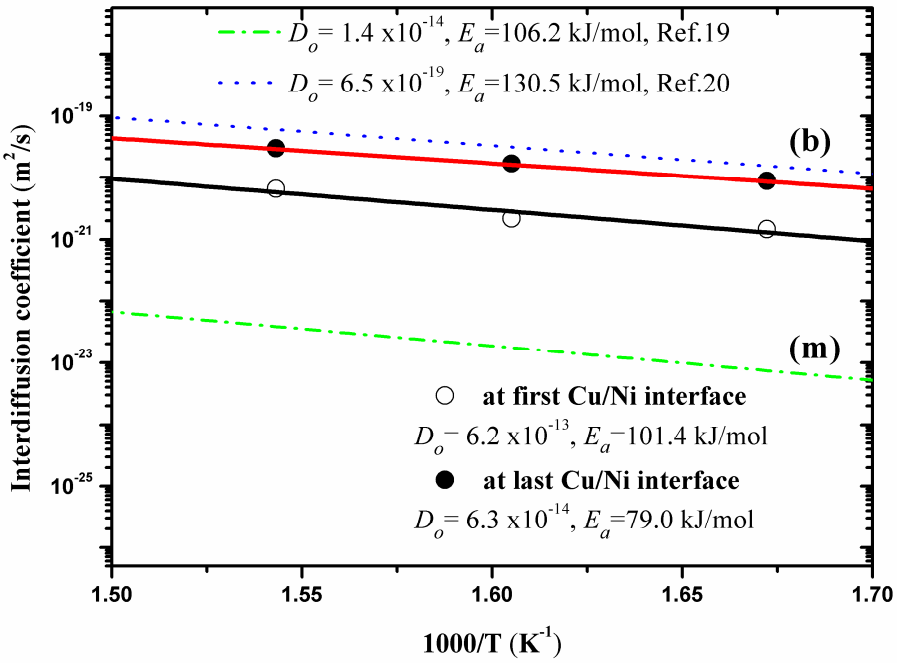

Figure 2. Arrhenius plots for the interdiffusion coefficients calculated from the fitted roughness parameters (see Fig. 1) by applying Eq. (1). The open and solid circles represent the values of the interdiffusion coefficient at the locations of the first and last Cu/Ni interface, respectively. The corresponding interdiffusion parameters (pre-exponential factor D_o and activation energy E_a) are indicated in bilayer (b) and multilayer (m) thin films.

Table 1. Diffusion parameters obtained in the present work in comparison with the results of other workers.

Source	D_o (m^2/s)	E_a (kJ/mol)
Present work (first Cu/Ni interface)	**6.2×10^{-13}**	**101.4**
Present work (last Cu/Ni interface)	**6.3×10^{-14}**	**79.0**
Ref.18	2×10^{-5}	228.7
Ref.19	1.4×10^{-14}	106.2
Ref.20	6.48×10^{-9}	130.5
Ref.21	6×10^{-12}	94.1
Ref.22	6.93×10^{-7}	90.4

The very low activation energy E_a values of 101.4 kJ/mol (79.0 kJ/mol) obtained in the present work in comparison with an E_a value of 228.7 kJ/mol extracted from a single crystalline copper [18], suggests that grain boundary and high defect density play a dominant role in the diffusion process of the

investigated multilayer thin films. The obtained diffusion parameters, measured at the low temperature range of 325-375 ºC, agree reasonably well with the ones listed in Table 1 for the polycrystalline bi-/multilayer films samples [19-22], which support the grain boundary diffusion mechanism at low temperatures for polycrystalline Cu/Ni .

A close examination of Fig. 2 reveals that the interdiffusion in a Cu/Ni multilayer was faster across the last Cu/Ni interface (near the substrate) than across the first Cu/Ni interface (near the surface) with a difference in activation energy value of 22.4 kJ/mol. In order to quantitatively evaluate the depth-dependent interdiffusion coefficient, Fig.3 shows the interdiffusion coefficient as a function of the sputtered depth for the same annealing time 30 min at the three different investigated annealing temperatures, on the basis of Eq. (1) with a linear dependence on depth adopted for σ_T (see above). The open circle, square, triangle and solid circles represent the values of the interdiffusion coefficient at the locations of the first, second, third and last Cu/Ni interfaces, respectively. It is found that the interdiffusion coefficient increase with the sputtered depth at the three different annealed temperature. This result is related to the reduction of the activation energy with sputtered depth for interdiffusion at the first, second, third and last Cu/Ni interfaces as 101.4 kJ/mol, 87.7 kJ/mol, 81.9 kJ/mol and 79.0 kJ/mol, respectively. The use of ion sputtering may involve changes in both the creation of vacancies, and energy of removed vacancies in the grain boundary and/or near grain boundary. During the sputtering process the larger concentration of vacancies at the deeper sputter depth might be created. This reduction of the activation energy with sputtered depth was also observed in Cu/Ag, Au/Ag, Pd/Au and Pd/Cu multilayer structure with AES measured by Bukaluk [15, 16]. In addition, enhanced grain boundary diffusion could be involved in the multilayer closer to the substrate; this however needs to be investigated further.

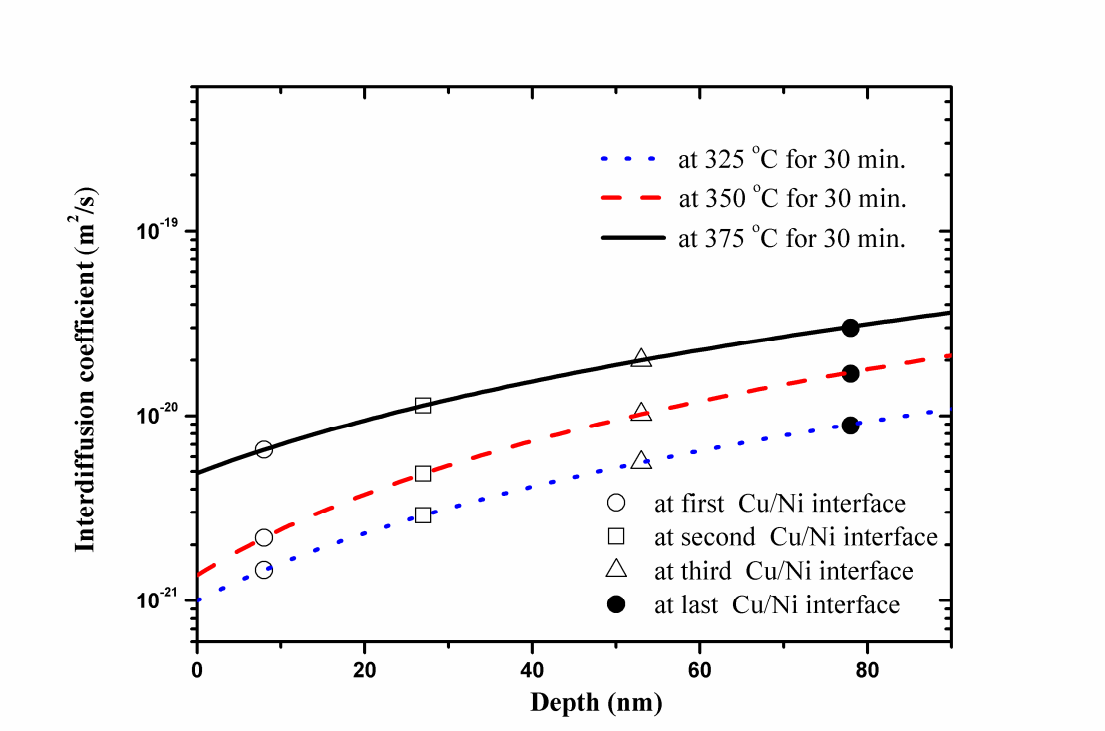

Figure 3. The interdiffusion coefficient as a function of the sputter depth for the annealed sample for 30 min at 325 ºC, 350 ºC and 375 ºC, respectively. The open circles, squares, triangles and solid circles represent the values of the interdiffusion coefficient at the locations of the first, second, third and last Cu/Ni interfaces, respectively.

4. Conclusions

The MRI model was applied for extracting the interdiffusion coefficients in Cu/Ni multilayers from measured AES depth profiling data. The interdiffusion coefficient of Cu/Ni multilayer was determined by $6.2\times10^{-13}\exp(-101.4\ kJ/RT)$ m^2/s at the first Cu/Ni interfaces and by $6.3\times10^{-14}\exp(-79.0\ kJ/RT)$ m^2/s m^2/s at the last Cu/Ni interfaces.

Acknowledgements

This work is based on the research supported by the South African Research Chairs Initiative of the Department of Science and Technology and National Research Foundation of South Africa. We would like to thank the National Research Foundation and the cluster of the University of the Free State for financial assistance.

References

[1] Jeon IJ, Hong JH and Lee YP 1994 *J. Appl. Phys.* **75** 7825
[2] Pretorius R, Marais TK and Theron CC 1993 *Mater. Sci. Eng. Rep.* **10** 1
[3] Bukaluk A 1983 *Surf. Interface Anal.* **5** 20
[4] Hall PM and Morabito JM 1976 *Surf. Sci.* **54** 79
[5] Highmore RJ, Evetts JE, Greer AL and Somekh RE 1987 *Appl. Phys. Lett.* **50** 566
[6] Pamler W 1987 *Appl. Phys.* A **42** 219
[7] Hofmann S 1994 *Surf. Interface Anal.* **21** 673
[8] Kesler V and Hofmann S 2002 *J. Surf. Anal.* **9** 428
[9] Wang JY, Zalar A, Zhao YH and Mittemeijer EJ 2003 *Thin Solid Films* **433** 92
[10] Wang JY, Zalar A and Mittemeijer EJ 2004 *Appl. Surf. Sci.* **222** 171
[11] Hedberg CL (by edited), *Handbook of Auger Electron spectroscopy, Third Edition,* Physical Electronics Industries, Eden Prairie, MN, USA,1976
[12] Ziegler JF, TRIM Code, IBM Corporation, Yorktown Heights, NY, (http:// www.srim.org)
[13] NIST Electron EAL, 2001 *NIST Database* 82
[14] Yan XL, Liu Y, Swart HC, Wang JY and Terblans JJ, Proceedings of SAIP2015. This volume.
[15] Bukaluk A 2001 *Vacuum* **63** 119
[16] Bukaluk A 2000 *Surf. Interface Anal.* **30** 597
[17] Wang JY, Hofmann S, Zalar A and Mittemeijer EJ 2003 *Thin Solid Films* **444** 120
[18] Van Dijk T and Mittemeijer EJ 1977 *Thin Solid Films* **41** 173
[19] Venos R, Pamler W and Hoffmann H, 1988 *Thin Solid Films* **162** 155
[20] Joubert HD, Terblans JJ and Swart HC 2010 *Surf. Interface Anal.* **42** 1281
[21] Abdul-Lettif AM 2007 *Phys.B* **388** 107
[22] Divinski S, Ribbe J, Schmitz G and Herzig C 2007 *Acta Mater.* **55** 3337